Tensile Properties of an Engineered Cementitious Composite Shotcrete Mix

Yi-Wei Lin[1], Liam Wotherspoon[2] & Jason M. Ingham[3] M.ASCE

CE Database Subject Headings: Fiber Reinforced Materials, Tensile Strength, Strain, Shotcrete

Abstract

Results are presented for a series of laboratory tests that were undertaken to characterise the tensile properties of an engineered cementitious composite (ECC) mix, which is a mortar-based composite reinforced with synthetic fibers to provide tensile strain-hardening characteristics. Dogbone, rectangular and circular bar shaped specimens were developed to determine the most suitable specimen geometry for uniaxial tensile testing (UTT), with the circular bar specimens that were constructed by coring through sprayed ECC panels showing the best geometrical consistency both within each specimen and between individual specimens. 50 circular bar specimens with a diameter of 16 mm and a length of 200 mm were tested under uniaxial tension to determine the characteristic tensile properties. Statistical distributions were used to define a 5% characteristic tensile yield strength of 1.82 MPa and a 10% tensile total strain of 0.08%. A material ductility factor of 4.0 was determined and k factors are proposed to convert quality assurance test mean values to characteristic values.

[1]PhD Candidate, Department of Civil and Environmental Engineering, University of Auckland, Private Bag 92019, Auckland, New Zealand, ylin126@aucklanduni.ac.nz.
[2]EQC Research Fellow, Department of Civil and Environmental Engineering, University of Auckland, Private Bag 92019, Auckland, New Zealand, l.wortherspoon@auckland.ac.nz
[3]Professor, Department of Civil and Environmental Engineering, University of Auckland, Private Bag 92019, Auckland, New Zealand, j.ingham@auckland.ac.nz.

Introduction

Engineered Cementitious Composite (ECC) is a mortar-based composite reinforced with polyvinyl alcohol (PVA) synthetic fibers, that exhibits a strain-hardening characteristic through the process of multiple micro-cracking, with the average crack widths typically less than 100 μm prior to reaching the ultimate compression strain (Kanda et al. 2003). Micro-cracking occurs because the matrix cracking strength is lower than the bond and tensile strength of the fibers embedded in the matrix, and when loaded, stress is transferred through fibers that bridge the cracks.

The two major types of ECC mix design are a cast mix, which refers to ECC that is used as a self-consolidating composite when it is poured into formwork (Kong et al. 2003), and a shotcrete mix, which refers to ECC that can be sprayed (Kim et al. 2003). ECC has been used as a repair material for concrete (Li et al. 2000), the replacement of concrete for bridge slabs (Kim et al. 2004) and for strengthening of masonry infilled walls (Kyriakides & Billington 2008).

Although ECC has previously been used in practical applications, currently only limited testing for the development of characteristic properties has been reported. Recent studies, such as that conducted by Yang et al. (2007), typically focus on the influence of mix designs rather than material property characterisation. The reported studies contain insufficient information to enable the development of engineering characteristic material properties that are necessary for a practical structural design procedure, and therefore systematic material testing of ECC was required to enable its use as a structural engineering material. This requirement was the motivation for the testing program outlined herein.

As the primary use of ECC is in the form of a tensile element, it can be used to retrofit structural elements or buildings that have insufficient tensile strength. Example applications of ECC for the seismic strengthening of unreinforced masonry (URM) buildings are reported in Lin et al. (2010). When strengthening URM buildings, ECC is typically applied onto masonry wall surfaces to improve the out-of plane and in-plane strength (Lin et al. 2011). To increase the out-of-plane wall flexural strength the ECC overlay resists the tension forces and the masonry wall resists the compression forces. To improve in-plane wall diagonal tension strength, the ECC overlay provides stress transfer over cracked wall sections and limits wall displacement. The two strengthening scenarios show that the tensile properties are critical in influencing the behaviour of the strengthened element and therefore are the most important parameters to be characterized.

The properties defined in this study are:

- Tensile yield strength
- Tensile ultimate strength
- Tensile ultimate strain
- Tensile total strain
- Tensile strength at tensile total strain
- Young's modulus

Figure 1 provides a graphical representation of the listed properties identified on the tensile stress strain response of an example specimen. Tensile yield strength refers to the strength where the tensile response transitions from an elastic response to a plastic response. Tensile ultimate strength is the maximum stress that can be sustained by the specimen and ultimate strain is the corresponding strain at this ultimate strength. Tensile total strain is the tensile

strain corresponding to a local maximum stress just prior to initiation of the strain-softening response, with the local maximum stress being higher than the tensile yield strength. Young's modulus is the gradient of the slope between tensile yield strength and the initial unloaded state. During strengthening design involving ECC, ECC tensile yield values and Young's modulus are used to predict the strengthened material response in the elastic phase and the strengthened composite section capacity. Tensile ultimate strength and strain values are used to anticipate the maximum strengthened composite section strength and to predict failure sequences of the composite wall and other connected structural elements. Determination of the tensile total strength and strain allows the quantification of the material ductility factor, which represents the ability of the material to undergo plastic deformation while maintaining a tensile strength beyond the tensile yield strength. Knowing the material ductility factor allows an improved prediction of the magnitude of the forces the strengthened elements will be subjected to, and in this study, material ductility factor is defined as the ratio of the tensile total strain to the tensile yield strain (ASCE/SEI 2007). Lastly, k factor is defined based upon a Gaussian distribution, which is used to convert mean values to characteristic values to ensure that the specified characteristic values are achieved even when only a small sample size is available.

For strength values, the lower 5% characteristic strength is typically used for design purposes (NZS 2001, JSCE 2008) and is the value that has been adopted here. To the authors' knowledge, no studies have indicated an appropriate percentage characteristic value that should be adopted for the tensile strain capacity of fiber reinforced concrete (FRC). Therefore, the approach used in this study was to adopt a lower 10% characteristic value for design purposes, which is a value that is typically reported for reinforcing steels according to NZS (2001) and CEN (1992). For Young's modulus, a 50% characteristic value is typically

used for design purposes (NRC 2006, NZS 2010), as both overestimation and underestimation of the structural deflection is undesirable. Table 1 summarises the material properties and the percentage of characteristic values that were investigated.

Mix proportions and procedures

The ECC mix tested in this study was supplied prebagged and was comprised of the materials and mix proportions listed in Table 2. These mix proportions are similar (in terms of the cement:sand:fly ash ratio, with identical fibre type but minor differences in additive dosage to account for local temperature variations) to those used by previous researchers around the world to repair concrete beams (Kim et al. 2004) and to strengthen unreinforced masonry buildings (Lin et al. 2010) and masonry elements (Kyriakides & Billington 2013).

Kaipara 425 sand was used with a maximum particle size of 425 μm, and the fly ash used was type F fly ash. The PVA fibers had a length of 8 mm, a diameter of 39 μm, and a tensile ultimate strength of 1620 MPa. Leung et al. (2005) showed that the material properties of sprayed FRC were significantly different to their cast counterparts having a similar composition. Therefore, to simulate the characteristics of actual application, the bagged materials were added to a two stage mixer and sprayed into boxes to form panels that were 1 m high × 1 m long × 100 mm thick. The panels were sprayed with water mist for seven days and then sealed with plastic wraps and cured under a constant temperature of 25±2ºC for 56 days.

Test specimens and setup

The uniaxial tensile test (UTT) method used in this study to characterise the tensile properties of ECC shotcrete was a modification of the test procedure reported by the Japan Society of Civil Engineering (JSCE 2008). A dogbone shaped test specimen (see Figure 2a) is used in

123 the JSCE test, where the ends of the test specimen have an increased width to provide a larger
124 bond area for the steel plates used to secure the specimen to the tensile testing apparatus. The
125 reduction in the width of the central region concentrates the stress and is ideal for limiting the
126 location of crack development. However, while existing steel molds for the dogbone shape
127 are available, the use of these molds is only practical for cast ECC mixes as spraying into the
128 relatively small molds prevents the ECC shotcrete from compacting properly at the recessed
129 edges. The European Federation of National Associations Representing Concrete (EFNARC)
130 (1996) suggests that any materials within 125 mm of the edge of a mold should not constitute
131 part of a test specimen. Therefore, the only published method available to produce the
132 specimens used for the JSCE (2008) test required an ECC panel to be sprayed and specimens
133 to then be cut out. Six dogbone shaped specimens were extracted from a panel using an angle
134 grinder, but difficulties were encountered during the cutting process due to the complex
135 shape, taking approximately one hour to produce each specimen. Additionally, the extracted
136 specimens were not geometrically consistent as every edge had to be cut individually and the
137 two edges of the central recessed region of the specimen were not of equal length in any of
138 the specimens. Because of this difficulty the specimens manufactured for testing using the
139 JSCE (2008) procedure were of insufficient regularity for use in this study, resulting in a non-
140 uniform stress distribution that influenced determination of the true tensile strength. To
141 simplify the specimen geometry, a rectangular shape (see Figure 2b) was used instead of the
142 dogbone shape to reduce the number of edges that had to be cut to produce each specimen.
143 Again difficulties were encountered in cutting and the cross-sections of the specimens had a
144 variability of ±5 mm both in width and thickness in comparison to the ideal dimensions.
145 Attempts were made to test the rectangular bars in uniaxial tension, but many of the
146 specimens failed in bending about the long axis of the rectangular cross-section rather than by
147 failing in pure tension due to the asymmetrical cross-section.

To avoid the difficulties involved in cutting out the specimens as described above, an alternative approach was adopted that involved coring out circular bar specimens (see Figure 2c) from the panels using a specialised core drill, with cores having a 16 mm diameter and a length of 500 mm. A similar approach was used by Barragan et al. (2003) to conduct UTT with cored samples extracted from steel fiber reinforced concrete. Cores were extracted perpendicular to the spray direction because for applications where ECC is used as a tensile-resisting element (such as strengthening of concrete beams (Kim et al. 2004)) and masonry walls to increase the flexural capacity (Lin et al. 2010), it is typically the ECC material tensile strength perpendicular to the spray direction that is critical in influencing the member capacity. The specimen diameter was selected based on considerations of ECC panel thickness available from field applications, which is typically 30 mm, and because 16 mm diameter was the maximum core size that could be extracted using the available core driller. This scenario resulted in edge distances during the coring operation of approximately 7 mm. The extracted bars were then trimmed and only the 200 mm central length was tested. The benefits of coring were that only a single cut through the core needed to be made and a consistent cross-sectional geometry was obtained along the length of the core. Measurements of the cross-sectional diameter taken along the length of the core showed a variation of ±0.2 mm from the ideal dimensions, which was significantly less deviation than the measured variability of the rectangular specimens.

A scatter of small voids was observed on the surface of the cored specimens, formed by air entrapped in the shotcrete during the spraying process. It should be noted that while these small voids may have a minor influence on the overall tensile properties over a large section of the shotcrete (such as when applied to an entire wall), these voids are likely to have had a

greater effect on the UTT specimens tested in this study due to the significantly smaller cross-sectional area of the specimens. Therefore, it is emphasised that the material properties obtained in this study are likely to be more conservative than those for test specimens with a larger cross-sectional area where the overall effect of these geometric irregularities is expected to reduce. Larger specimens were not adopted in this study as increasing the cross-sectional area would have introduced additional testing issues such as the requirement of a larger bond area between the specimen and the loading apparatus, and the need for a greater amount of material to produce the same number of specimens.

Once the most practical specimen shape had been defined, it was necessary to determine an appropriate method to secure the ends of the specimens to the testing apparatus. The frictional grips that are typically used for steel bar tensile testing were deemed unsuitable because of the possibility of localized crushing of the specimen. Instead a method similar to that used by Kocaoz et al. (2005) and Lorenzis & Nanni (2001) to grip glass fiber reinforced polymer (GFRP) bars was adopted, where steel tubes were slotted over the bar ends and the gap between the bar and the tube was filled with expandable cementitious grout to provide a confining pressure. In this study, a threaded insert (a steel tube with internal threads that are typically used to connect reinforcing bars) was attached to each end of the specimen, and the gap was filled with an expansive epoxy. Two rubber bearings were placed inside each threaded insert to ensure that the centre of the specimen was aligned with the centre of the threaded insert, as any misalignment would have induced eccentricities and created bending moments when the extracted core was subjected to tension. Each end of the specimen was connected via a pin to a 100 kN Instron machine, and two LVDTs were attached to either side of the specimen to measure the extension over the central 70% of the specimen length. This LVDT gauge length was used in the calculation of material strain. Figure 3 shows a

198 schematic representation of the setup. Fifty specimens were tested to determine the
199 characteristic property values, with the sample size selected based on a similar study
200 conducted by JSCE (2008), where 49 specimens were tested to determine the characteristic
201 properties of cast ECC mixes. An example of a tested specimen is shown in Figure 4a, with
202 Figure 4b showing that cracks typically developed perpendicular to the specimen length due
203 to the uni-axial tension applied to the specimen.
204
205 **Results**
206 *Statistical distribution models and analysis*
207 To determine the characteristic values of the ECC shotcrete mix from the specimen data
208 collected, it was necessary to determine a statistical distribution model that could represent
209 the sample data. Normal, lognormal and Weibull distributions were selected as potential
210 distribution models that could represent the material property distribution obtained in this
211 study. These three models were selected because they are commonly used for characterising
212 material properties in structural engineering. Each of the distribution types have been used by
213 Bernard et al. (2010), Zureick et al. (2006), Lorenzis & Nanni (2001) and Kocaoz et al.
214 (2005) in various statistical studies on material properties.
215
216 A normal distribution has a bell-shaped curve that is symmetrical about the mean of the
217 population, and was previously used to represent concrete material properties (MacGregor et
218 al., 1983), to represent the distribution of tensile strength of GFRP (Kocaoz et al., 2005), and
219 for assessing the flexural and compressive strength of carbon fiber reinforced concrete
220 (Soroushian et al., 1992). A lognormal distribution is typically skewed towards one end of the
221 distribution instead of being symmetrical about the mean. Lognormal distributions are often
222 observed for steel material property distributions, such as in the study conducted by

223 Galambos et al. (1982), and in this study a two parameter distribution was adopted for data
224 modelling. A Weibull distribution is fundamentally different to normal and lognormal
225 distributions. For normal and lognormal distributions, the data is fitted and tested against a
226 predefined distribution type, whereas a Weibull distribution has a scale and shape factor that
227 allows it to be fitted to data with more flexibility. Weibull distributions have been used by
228 ASCE (1996) to represent the property distributions of timber materials and by Toutanji et al.
229 (1994) to represent the tensile properties of carbon fiber reinforced concrete.
230
231 Statistical analyses were conducted using R, which is a non-commercial statistical analysis
232 having a large international user base (R Foundation 2012). The Anderson-Darling test was
233 used to test the goodness of fit of the probability distribution selected, as this test is sensitive
234 to the lower end of the distribution (Lawless 1982), which was the focus of this study seeking
235 to define the characteristic material properties. The null hypothesis (H_0) of the
236 Anderson-Darling test is that the test values fit the probability distribution type selected, and
237 the p-value of the test will indicate whether there is any evidence against the null
238 hypothesis. Higher p-values indicate a higher probability that if more samples were
239 tested, the additional data would follow the same type of distribution as exhibited in this
240 study (Fisher 1925) and a p-value less than 0.05 typically indicates that the selected
241 distribution model does not fit the data distribution (Fisher 1926).
242
243 *Tensile strength*
244 The tensile yield strength, tensile ultimate strength, and tensile strength at tensile total strain
245 of each of the tested ECC shotcrete specimens are summarised in Table 3. The resulting p-
246 values for the distribution models fitted to the test data are shown in Table 4. For tensile yield
247 strength both the normal distribution and a positively skewed lognormal distribution resulted

248 in p-values in excess of 0.100, indicating an acceptable fit between the theoretical distribution
249 and the distribution of the test data. The lognormal distribution was adopted as the p-value of
250 0.625 was higher than the p-value of 0.220 from the normal distribution fitting. Using the
251 lognormal distribution model, the 5% characteristic tensile yield strength was equal to
252 1.82 MPa. For tensile ultimate strength, again both the normal distribution and a positively
253 skewed lognormal distribution resulted in p-values in excess of 0.100, with the lognormal
254 distribution having the highest p-value. Adopting the lognormal distribution resulted in a 5%
255 characteristic tensile ultimate strength of 2.64 MPa. The tensile strength at tensile total strain
256 (strain prior to the initiation of a strain-softening behaviour) was best represented by a normal
257 distribution, with the 5% characteristic value equal to 2.26 MPa. Figure 5 shows the
258 lognormal distribution model fitted to the tensile yield strength, tensile ultimate strength and
259 the normal distribution model fitted to the tensile strength at tensile total strain data.
260
261 *Tensile strain, Young's modulus*
262 The measured tensile strain values were analysed following the same methodology as was
263 used for the strength data, with the outputs summarised in Table 4 and results from all tests
264 listed in Table 3. Both a positively skewed lognormal distribution and Weibull distribution
265 fitted the ultimate strain distribution, with the lognormal distribution having the highest p-
266 value. Adopting the lognormal distribution type resulted in a 10% characteristic tensile
267 ultimate strain of 0.07%. For the tensile total strain (strain prior to softening behaviour) the
268 Weibull distribution had the best fit to the sample data and the resulting 10% characteristic
269 tensile total strain was 0.08%. Figure 6a and Figure 6b present the cumulative distribution
270 curves of the distribution models fitted to the tensile strain results. For Young's modulus, all
271 three distribution types fitted the data set, with the lognormal distribution resulting in the
272 highest p-value of 0.983 and therefore used to derive the 50% characteristic Young's

modulus of 9.5 GPa. Figure 6c shows the lognormal distribution model fitted to the Young's modulus data. The variability in the calculated Young's modulus was attributed to air voids within each specimen that formed during the spraying process. Similar variability is expected to be encountered in field applications due to the absence of a technique available for reducing voids such as is available for conventional casting. Adoption of larger diameter specimens in future investigation may decrease the influence of air voids and consequently reduce variability of the derived Young's modulus.

Characteristic tensile response and material ductility factor

Using the characteristic values for each of the tensile properties determined from the distribution models, the expected characteristic tensile response of the ECC shotcrete mix is plotted in Figure 7 and is compared to the tensile response of all specimens. Figure 7 shows that the majority of the ECC specimens exhibited a response that exceeded the proposed characteristic response.

As ECC shotcrete is expected to be used as a form of tensile reinforcement, the ductility of the material (material ductility factor) is important as it influences the level of seismic acceleration that an ECC shotcrete reinforced structure will be subjected to during an earthquake (Agarwal and Shrikhande 2006). The material ducility factor is dependant on the tensile yield strain and tensile total strain, and by substituting the known values from Table 5 into Equation 1 and 2, the material ductility factor of ECC is equal to 4.0.

$$Tensile\ yield\ strain = \frac{Lower\ 5\%\ characteristic\ tensile\ yield\ strength}{50\%\ characteristic\ Young's\ modulus} = \frac{1.82}{9.5 \times 10^3} \times 100 = 0.02\% \quad (1)$$

$$Material\ ductility\ factor = \frac{Lower\ 10\%\ characteristic\ tensile\ total\ strain}{Tensile\ yield\ strain} = \frac{0.08\%}{0.02\%} = 4.0 \quad (2)$$

295

296 *Population standard deviation for tensile yield strength*

297 Bernard et al. (2010) have previously demonstrated that the coefficient of variance (equal to
298 the standard deviation (σ) divided by the mean) derived from testing of a limited number of
299 specimens is not representative of the true coefficient of variance of the population. They
300 showed that the relationship between the coefficient of variance (CoV) and the number of
301 specimens tested resembled a logarithmic curve, with the CoV increasing rapidly as a larger
302 number of specimens were tested and eventually becoming stable (in the Bernard et al.
303 (2010) study the results became stable after the number of test specimens exceeded ten). As
304 the quality assurance (QA) testing performed on site is unlikely to have a sufficient number
305 of samples to determine the population standard deviation, and therefore insufficient
306 information will be available to confirm whether the tested specimens have achieved the
307 specified characteristic strength, it was deemed necessary to analyse the change in the σ
308 obtained from this study against the number of specimens tested. This requirement is because
309 CoV is a function of σ and it is expected that the value of σ will be influenced by the sample
310 size. Studies by Soroushian et al. (1992) and Nataraja et al. (1999) recommended either a
311 large number of tests to ensure that the material properties determined from testing conform
312 with specified characteristic values, or that the σ obtained from an existing large sample of
313 tests be adopted when assessing the material properties derived from a smaller sample size,
314 subject to the condition that the σ obtained from the smaller sample size is of similar value.

315

316 The relationship between the σ of the tensile yield strength for a reduced sample set to the σ
317 obtained from the total sample size (50 specimens) is plotted in Figure 8, where the results
318 obtained from testing were randomly ordered and the σ calculated. This process was repeated
319 100 times to produce the final averaged relationship. Figure 8 shows that the σ values

increased significantly over the first 12 specimens, being slightly higher than the number of panels (ten) that Bernard et al. (2010) had to test before the σ began to stabilise, with a maximum measured σ of 0.23 MPa and a CoV of 0.23. The increase in the number of specimens required for a stable σ in this study was most likely attributed to the higher variability of the properties of the sprayed specimens as opposed to Bernard's cast panels. Additionally, the properties measured in this study were obtained from UTT tests, which were regarded in studies conducted by Stang & Li (2004), Ostegaard et al. (2005) and Kanakubo (2006) as a highly complicated and delicate test method, adding further variability in the properties measured.

While the σ fluctuates considerably when more specimens are tested, the mean value of the tensile yield strength was shown to be relatively consistent after sampling just eight specimens (see Figure 8). This observation corresponds with observations made by Bernard et al. (2010) where the mean values of the sample were less sensitive to the number of specimens tested. Knowing that the mean of the samples tested remains relatively consistent as long as a reasonable number of specimens are available (such as ten), but that the σ requires significantly more specimens to be sampled in order to ensure that the maximum σ is obtained, there is a need for a method to ensure that if a limited amount of samples were tested, the expected lower characteristic value can be predicted.

Conversion of mean values to characteristic values using k factor

Equation 3 is used by JSCE (2008) for conversion of mean values to characteristic values for normally distributed material properties, where k is determined by the probablity of the tested sample mean value falling below the charactertistic value (for either 5% or 10% lower characteristics value, depending on whether the parameter of interest is strength or strain).

$$Characteristic\ value = mean\ value - k \times standard\ deviation \quad (3)$$

As the lower characteristic value, mean value and standard deviation can all be established from the test data, k can be calculated by rearranging Equation 3. This exercise was undertaken in order to compare experimental results against the true theoretical value. The available data was processed for the material properties that were normally distributed, and for material properties that were lognormally distributed a normal distribution was applied to the natural log values of the original data to calculate the k factor.

The calculated k factors are presented in Table 6 and it is recommended that Equation 4 should be used to check that the QA samples exceed the specified design characteristic values. Unless a large amount of QA test results are available the standard deviation (σ) should be taken as 0.23×QA sample mean value if the sample size is less than 12, and a minimum of ten specimens should be tested for QA purposes.

$$QA\ sample\ mean\ value - k\sigma \geq specified\ characteristic\ properties \quad (4)$$

Recommendations for further research

The current investigation was conducted using 16 mm diameter ECC cores. It is recommended that further investigation be conducted on the influence of specimen diameter on the material properties.

Conclusions

In this study 50 circular bar specimens were tested to determine characteristic tensile material properties of an ECC shotcrete mix. Circular bar shaped specimens were shown to be the most practical shape for tensile testing as they had the least specimen dimensional variability when compared with dogbone and rectangular shaped specimens. Three distribution models were used to represent the material property values examined and the following values provide an indication of typical design values if the investigated ECC shotcrete mix is reproduced and tested using a similar method:

- 5% characteristic tensile yield strength = 1.8 MPa
- 5% characteristic tensile ultimate strength = 2.6 MPa
- 5% characteristic tensile strength corresponding to tensile total strain = 2.3 MPa
- 10% characteristic tensile ultimate strain = 0.07%
- 10% characteristic tensile total strain = 0.08%
- 50% Young's modulus = 9.5 GPa
- Material ductility factor = 4.0

The results of this study showed that as the number of tested specimens increased, the standard deviation increased rapidly and stabilised after 12 samples were tested, with a final standard deviation of 0.23 MPa and a CoV of 0.23. It is recommended that a minimum standard deviation of 0.23×QA sample mean value be applied to the tensile yield strength from quality assurance specimens produced on site when the total number of samples tested is less than 12, subject to the ECC mix being identical to that reported in this study and tested using the reported method. A minimum of ten specimens is suggested for QA testing purposes to ensure that the true characteristic tensile yield strength of the QA specimens

exceeds the specified characteristic tensile yield strength. Using this data, k factors have been proposed to convert sample mean values to the expected characteristic values.

Acknowledgements

The authors wish to acknowledge Royce Finlayson, Michael Ryan, Bing Zhang, Karl Yuan and Anthony Le Dain for their assistance in sample production, preparation and testing. The authors would also like to thank Derek Lawley, David Nevans, Michael Barry and Roydon Gilmour from Reid Construction Systems for providing some of the equipment required for this study. Lastly, the authors would like acknowledge the financial support of The New Zealand Ministry of Science and Innovation and the New Zealand Earthquake Commission.

402 **References**

403 Agarwal, P. and Shrikhande, M. (2006). "Earthquake Resistant Design of Structures."
404 New Delhi, India, Prentice-Hall of India Pvt. Ltd.
405
406 ASCE (1996). "Standard for Load and Resistance Factor Design LRFD for Engineered Wood
407 Construction." ASCE Standard 16-95, American Society of Civil Engineers, Virginia, United
408 State of America.
409
410 ASCE/SEI 7-05 (2005). "Minimum Design Loads for Buildings and Other
411 Structures." ASCE/SEI 7-05, American Society of Civil Engineers, Virginia, United State of
412 America.
413
414 Barragan, B. E., Gettu, R., Martin, M. A. and Zerbino, R. (2003). "Uniaxial Tension Test for
415 Steel Fiber Reinforced Concrete - A Parametric Study." *Cement and Concrete Composites*,
416 25(7): 767-777.
417
418 Bernard, E. S., Xu, G. G. and Carino, N.J. (2010). "Influence of the Number of Replicates in
419 a Batch on Apparent Variability in FRC and FRS Performance Assessed using ASTM C1550
420 Panels." *Proceedings of the 3rd International Shotcrete Conference*, Queenstown, New
421 Zealand, 15-17 Mar. CRC Press.
422
423 CEN (1992). "Eurocode 2 - Design of Concrete Structures." Eurocode 2: 1-225.
424 European Committee for Standardisation, Brussels, Belgium.
425
426 EFNARC (1996). "European Specification for Sprayed Concrete." EFNARC: 1-35. European
Federation of National Associations Representing Concrete, Surrey, United Kingdom.

Fisher, R. A. (1925). *Statistical Methods for Research Workers.* Oliver and Boyd, Edinburgh, UK.

Fisher, R. A. (1926). "The Arrangement of Field Experiments" *Journal of the Ministry of Agriculture Great Britain*, 33:503-513.

Galambos, T. V., Ellingwood, B., MacGregor, J. G. and Cornell, C. A. (1982). "Probability Based Load Criteria: Assessment of Current Design Practice." *Journal of Structural Division, American Society of Civil Engineering*, 108(5): 959–977.

JSCE (2008). "Recommendations for Design and Construction of High Performance Fiber Reinforced Cement Composites with Multiple Fine Cracks (HPFRCC)." JSCE**:** 1-88. Japan Society of Civil Engineers, Japan.

Kanakubo, T. (2006). "Tensile Characteristics Evaluation Method for Ductile Fiber-Reinforced Cementitious Composites." *Journal of Advanced Concrete Technology*, 4(1): 3-17.

Kanda, T., Saito, T., Sakata, N. and Hiraishi, M. (2003). "Tensile and Anti-Spalling Properties of Direct Sprayed ECC." *Journal of Advanced Concrete*, 1(3): 269-282.

Kim, Y. Y., Fischer, G. and Li, V. C. (2004). "Performance of Bridge Deck Link Slabs Designed with Ductile Engineered Cementitious Composite." *ACI Structural Journal*, 101(6): 792-801.

Kim, Y. Y., Kong, H. and Li, V. C. (2003). "Design of Engineered Cementitious Composite Suitable for Wet-Mixture Shotcreting." *ACI Materials Journal,* 100(6): 511-518.

Kim, Y., Fischer, G., Lim, Y. and Li, V. (2004). "Mechanical Performance of Sprayed Engineered Cementitous Composite using Wet-mix Shotcreting Process for Repair Applications." *ACI Materials Journal,* 101(1): 42-49.

Kyriakides, M. A. and Billington, S. A. (2013). "Strengthening of Masonry Using Sprayed Strain Hardening Cement-Based Composites (SHCC)." *Seventh RILEM Symposium on HPFRCC,* Chennai (Madras), India. 17-19 Sep.

Kocaoz, S., Samaranayake, V. A. and Nanni, A. (2005). "Tensile Characterization of Glass FRP bars." *Composites Part B: Engineering,* 36(2): 127-134.

Kong, H. J., Bike, S. G. and Li V. C. (2003). "Constitutive Rheological Control to Develop a Self-Consolidating Engineered Cementitious Composite Reinforced with Hydrophilic Polyvinyl Alcohol Fibers." *Cement and Concrete Composites,* 25(3): 333-341.

Kyriakides, M. A. and Billington S. L. (2008). "Seismic Retrofit of Masonry-Infilled Non-Ductile Reinforced Concrete Frames Using Sprayable Ductile Fiber-Reinforced Cementitous Composites." *The 14th World Conference on Earthquake Engineering*. Beijing, China. 12-17 Oct.

476 Lawless, J. F. (1982). “Statistical Models and Methods for Lifetime Data.” Wiley. New York,
477 United State of America.
478
479 Leung, C. K. Y., Lai, R. and Lee, A. Y. F. (2005). “Properties of Wet-Mixed Fiber
480 Reinforced Shotcrete and Fiber Reinforced Concrete with Similar Composition.” *Cement and*
481 *Concrete Research*, 35(4): 788-795.
482
483 Li, V. C., Horii, H., Kabele, P., Kanda, T. and Lim, Y. (2000). “Repair and Retrofit with
484 Engineered Cementitious Composites.” *Engineering Fracture Mechanics*, 65(2-3): 317-334.
485
486 Lin, Y., Lawley, D. Wotherspoon, L and Ingham, J. M. (2010). “Seismic Retrofitting of an
487 Unreinforced Masonry Building Using ECC Shotcrete.” *New Zealand Concrete Industry*
488 *Conference*. Wellington, New Zealand. 7-9 Oct.
489
490 Lin, Y., Derakhshan, H., Dizhur, D., Lumantarna, R. Wotherspoon, L. and Ingham J.
491 M. (2011). “Testing and Seismic Retrofit of 1917 Wintec F Block URM Building in
492 Hamilton.” *SESOC*, 24(1): 47-57.
493
494 Lorenzis, L. D. and Nanni, A. (2001). “Characterization of FRP Rods as Near-Surface
495 Mounted Reinforcement.” *Journal of Composites for Construction*, 5(2): 114-121.
496
497 Maalej, M., Lin, V. W. J., Nguyen, M. P. and Quek, S. T (2010). “Engineered Cementitious
498 Composites for Effective Strengthening of Unreinforced Masonry Walls.” *Engineering*
499 *Structures* 32(8): 2432-2439.
500

MacGregor, J. G., Mirza, S. A. and Ellingwood, B. (1983). "Statistical Analysis of Resistance of Reinforced and Prestressed Concrete Members." *Journal of American Concrete Institute,* 80(3), 167–176.

Nataraja, M. C., Dhang, N. and Gupta, A. P. (1999). "Statistical Variations in Impact Resistance of Steel Fiber-Reinforced Concrete Subjected to Drop Weight Test." *Cement and Concrete Research*, 29(7): 989-995.

NRC (2006). "Guide for the Design and Construction of Fiber-Reinforced Concrete Structures." CNR-DT 204/2006: 1-55. National Research Council, Rome, Italy.

NZS (2001). "Steel Reinforcing Materials." NZS 4671:2001: 1-43. New Zealand Standards, Wellington, New Zealand.

NZS (2010). "Characterization of Structural Timber." NZS 4603:2010: 1-80. New Zealand Standards, Wellington, New Zealand.

Ostergaard, L., Walter, R. and Olesen, J. F. (2005). "Method for Determination of Tensile Properties of Engineered Cementitious Composites (ECC)." *Conference on Construction Materials*. Vancouver, Canada. 22-24 Aug.

R Foundation. (2012). "The R Foundation for Statistical Computing." Retrieved 5th Dec, 2012, from http://www.r-project.org/foundation/main.html.

525 Soroushian, P., Nagi, M. and Alhozaimy, A. (1992). "Statistical Variations in the Mechanical
526 Properties of Carbon Fiber Reinforced Cement Composites." *ACI Materials Journal*, 80(2):
527 131-138.
528
529 Stang, H. and Li, V. C. (2004). "Classification of Fiber Reinforced Cementitious Material for
530 Structural Applications." *Sixth Rilem Symposium on Fiber Reinforced Concrete*, Varenna,
531 Italy. 20-22 Sep.
532
533 Toutanji, H. A., El-Korchi, T. and Katz, R. N. (1994). "Strength and Reliability of Carbon-
534 Fiber-Reinforced Cement Composites." *Cement and Concrete Composites*, 16(1): 15-21.
535
536 Yang, E. H., Yang, Y. and Li, V. C. (2007). "Use of High Volume Fly Ash to Improve ECC
537 Mechanical Properties and Material Greenness." *ACI Materials Journal* 104(6): 620-628.
538
539 Zureick, A. H., Bennett, R. M. and Ellingwood B. R. (2006). "Statistical Characterization of
540 Fiber-Reinforced Polymer Composite Material Properties for Structural Design." *Journal of*
541 *Structural Engineering, American Society of Civil Engineering,* 132(8): 1320-1327.
542
543
544
545
546
547
548
549

List of Tables

List of Figures

577

578

579

Table 1: Material characteristics defined in this testing program

Values to be determined	Notes
5% characteristic tensile yield strength	95% of population will achieve this value
5% characteristic tensile ultimate strength	95% of population will achieve this value
5% characteristic tensile strength corresponding to tensile total strain	95% of population will achieve this value
10% characteristic tensile ultimate strain	90% of population will achieve this value
10% characteristic tensile total strain	90% of population will achieve this value
50% Young's modulus	50% of population will achieve this value
k factor	A factor that is used to convert the sample mean value to the characteristic value
Material ductility factor	Ratio of tensile total strain to tensile yield strain

580

581

582

583

584

585

586

587

588

589

590

591

592

593

594

595

596

597

598

Table 2: Mix proportions of ECC tested

Materials	Proportions (kg/m^3)
Sand	640
Portland cement	760
Calcium Aluminate (CA) cement	40
Fly ash	240
Water	374
Super Plasticiser	2.6
Rheology Stabiliser	0.41
Fibers	2.6

599

600

601

602

603

604

605

606

607

608

609

610

611

612

613

614

615

616

617

Table 3: Material tensile properties for individual samples

Sample number	Tensile yield strength (MPa)	Tensile ultimate strength (MPa)	Tensile strength at tensile total strain (MPa)	Tensile ultimate strain (%)	Tensile total strain (%)	Young's modulus (GPa)
1	4.05	5.64	5.64	0.13	0.13	15.40
2	3.12	5.10	4.61	0.14	0.42	10.54
3	2.22	3.48	3.00	0.55	0.70	7.87
4	3.52	5.13	5.13	0.13	0.13	9.29
5	3.46	4.60	4.04	0.29	0.40	5.63
6	5.79	5.79	5.79	0.02	0.02	29.48
7	3.31	4.78	4.49	0.08	0.30	20.26
8	2.82	3.86	3.15	0.22	0.40	9.07
9	2.89	4.27	4.27	0.71	0.71	15.60
10	2.25	3.87	3.87	0.79	0.79	9.69
11	2.51	3.15	2.87	0.40	0.65	5.97
12	2.07	3.92	3.92	0.79	0.79	15.53
13	3.25	4.07	4.07	0.19	0.19	8.03
14	2.06	3.03	2.85	0.19	0.38	3.82
15	2.60	3.48	3.42	0.08	0.13	6.74
16	2.35	3.11	2.89	0.12	0.15	27.71
17	2.88	3.92	3.92	0.64	0.64	5.37
18	1.90	3.20	3.20	0.16	0.16	4.88
19	2.03	3.39	3.28	0.48	0.56	7.70
20	3.37	3.51	3.51	0.19	0.19	11.28
21	2.58	3.08	3.08	0.09	0.09	13.47
22	2.05	3.66	3.09	0.32	0.56	5.61
23	2.51	4.00	3.98	1.29	1.35	11.02
24	2.70	3.12	3.03	0.15	0.24	24.49
25	3.77	3.92	3.92	0.14	0.14	10.99

618

619

620

621

622

623

624

625

626

Table 3 continued: Material tensile properties for individual samples

Sample number	Tensile yield strength (MPa)	Tensile ultimate strength (MPa)	Tensile strength at tensile total strain (MPa)	Tensile ultimate strain (%)	Tensile total strain (%)	Young's modulus (GPa)
26	3.09	3.37	3.33	0.16	0.19	10.87
27	2.75	3.40	3.28	0.23	0.50	26.94
28	3.31	4.00	4.00	0.72	0.72	13.70
29	2.10	3.20	2.72	0.13	0.21	4.29
30	2.51	2.95	2.90	0.33	0.55	4.06
31	2.15	3.51	3.27	0.21	0.40	5.95
32	2.53	3.51	3.49	0.78	0.79	3.63
33	2.37	3.65	3.27	0.40	0.53	6.67
34	2.35	3.37	3.32	0.60	0.60	7.74
35	2.57	5.04	4.74	0.21	0.31	10.73
36	2.73	5.24	4.58	0.15	0.25	23.80
37	3.66	5.24	5.06	0.16	0.20	14.11
38	3.46	4.11	4.01	0.21	0.22	11.84
39	2.15	2.67	2.45	0.77	0.95	5.66
40	3.75	3.93	3.93	0.09	0.09	21.65
41	2.73	2.87	2.87	0.02	0.02	11.51
42	2.11	3.23	3.23	0.25	0.25	4.97
43	2.52	3.29	3.29	0.33	0.33	19.00
44	1.99	3.65	3.01	0.36	0.60	14.71
45	2.09	3.53	3.53	0.18	0.18	13.14
46	2.46	3.07	3.07	0.15	0.15	2.99
47	2.70	3.11	3.11	0.09	0.09	8.30
48	1.95	2.56	2.17	0.16	0.52	10.22
49	2.05	2.37	2.37	0.27	0.27	6.62
50	3.03	3.13	3.13	0.08	0.08	4.04

627

628

629

630

631

632

633

634

Table 4: p-values for tensile properties from each distribution models

distribution type	Tensile values analysed and the resulting p-values					
	Tensile yield strength	Tensile ultimate strength	Tensile strength at tensile total strain	Tensile ultimate strain	Tensile total strain	Young's modulus
Normal	0.220	0.162	0.244	0.015	0.264	0.119
Lognormal	0.625	0.457	1.2×10^{-5}	0.666	0.528	0.983
Weibull	1.2×10^{-5}	0.013	0.042	0.156	0.871	0.201

Table 5: Statistical tensile property values obtained from distribution modelling

	Characteristic value*
Tensile yield strength (MPa)	1.82
Tensile ultimate strength (MPa)	2.64
Tensile strength corresponding to tensile total strain (MPa)	2.26
Tensile ultimate strain (%)	0.07
Tensile total strain (%)	0.08
Young's modulus (GPa)	9.5

*5% for strength values, 10% for strain values, 50% for Young's modulus

Table 6: Statistical values of the various tensile properties used to derive the k factors

	Tensile yield strength	Tensile ultimate strength	Tensile strength at tensile total strain	Tensile ultimate strain	Tensile total strain
Distribution model	Lognormal	Lognormal	Normal	Lognormal	Weibull
Mean value	2.66 (0.98)	3.67 (1.30)	3.58	0.22 (-1.51)	0.39
Characteristic value	1.82 (0.60)	2.64 (0.97)	2.26	0.07 (-2.61)	0.08
Standard deviation	1.26 (0.23)	1.22 (0.20)	0.80	2.36 (0.86)	0.28
k factor (experimental)	1.65	1.65	1.65	1.28	N/A
k factor (theoratical)			1.65		

*Bracketed values presented here are log transformed values

691

Figure 1: Overview of the tensile properties investigated in this study

692

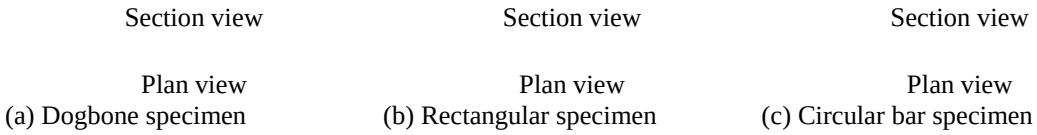

(a) Dogbone specimen (b) Rectangular specimen (c) Circular bar specimen

Figure 2: Tensile test specimen geometries

693

694

Figure 3: UTT setup of the ECC circular bar specimens

695

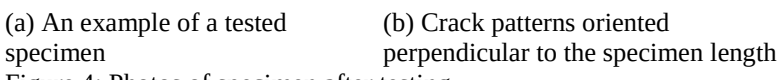

(a) An example of a tested specimen (b) Crack patterns oriented perpendicular to the specimen length

Figure 4: Photos of specimen after testing

696

(a) Tensile yield strength and lognormal distribution

(b) Tensile ultimate strength and lognormal distribution

(c) Tensile strength at tensile total strain and normal distribution

Figure 5: Cumulative distribution curve of tensile strengths from test data and corresponding distribution

697

(a) Tensile ultimate strain and lognormal distribution

(b) Tensile total strain and Weibull distribution

(c) Young's modulus and lognormal distribution

Figure 6: Cumulative distribution curve of tensile strains and Young's modulus from test data and corresponding distribution

698

Figure 7: ECC tensile characteristic response and tensile response of all tested specimens

699

Figure 8: Effect of specimen sample size on tensile yield strength mean and standard deviation

700

701

Figure 1
Click here to download Figure: Figure 1.pdf

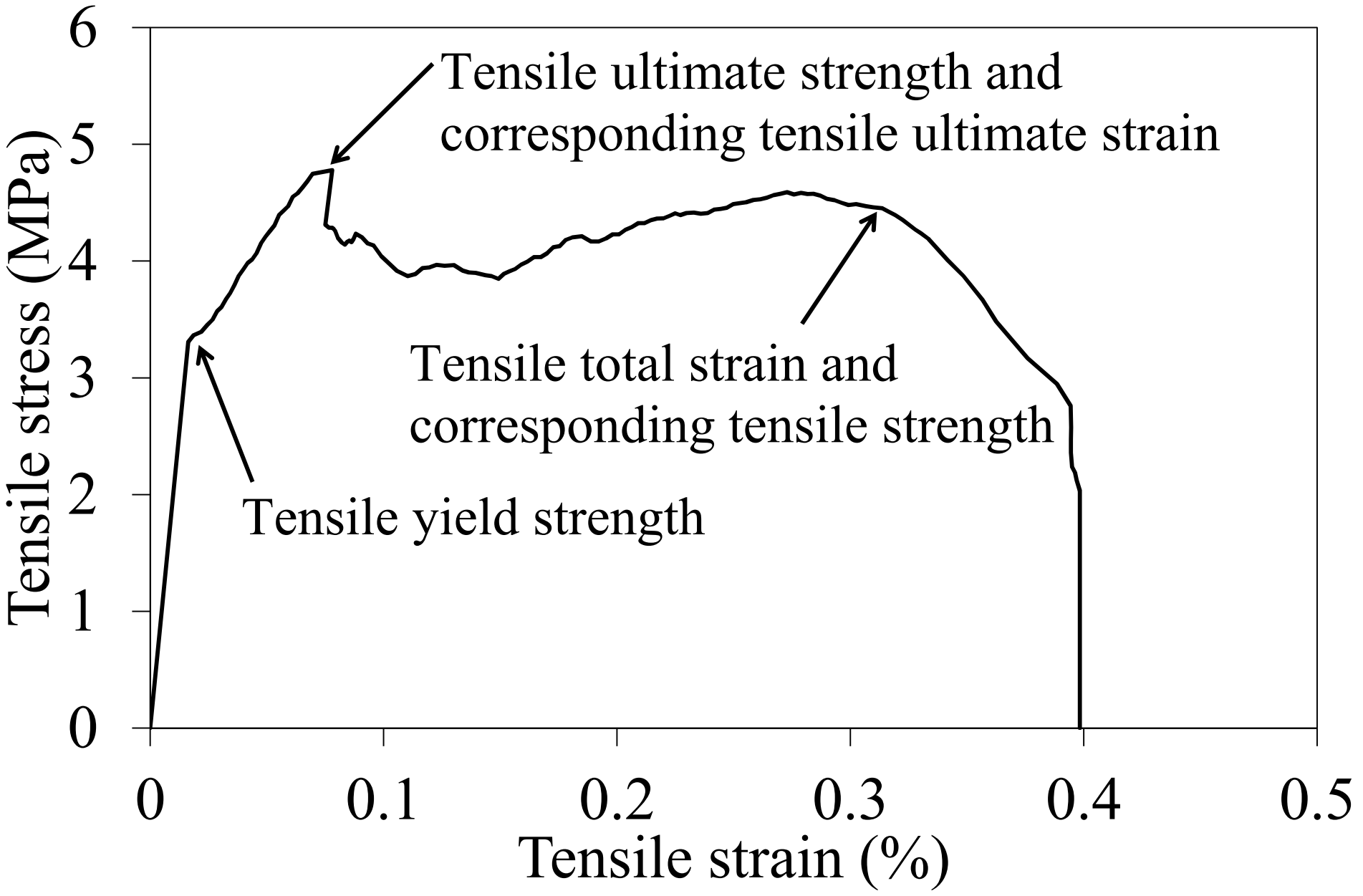

Figure 2a
Click here to download Figure: Figure 2a.pdf

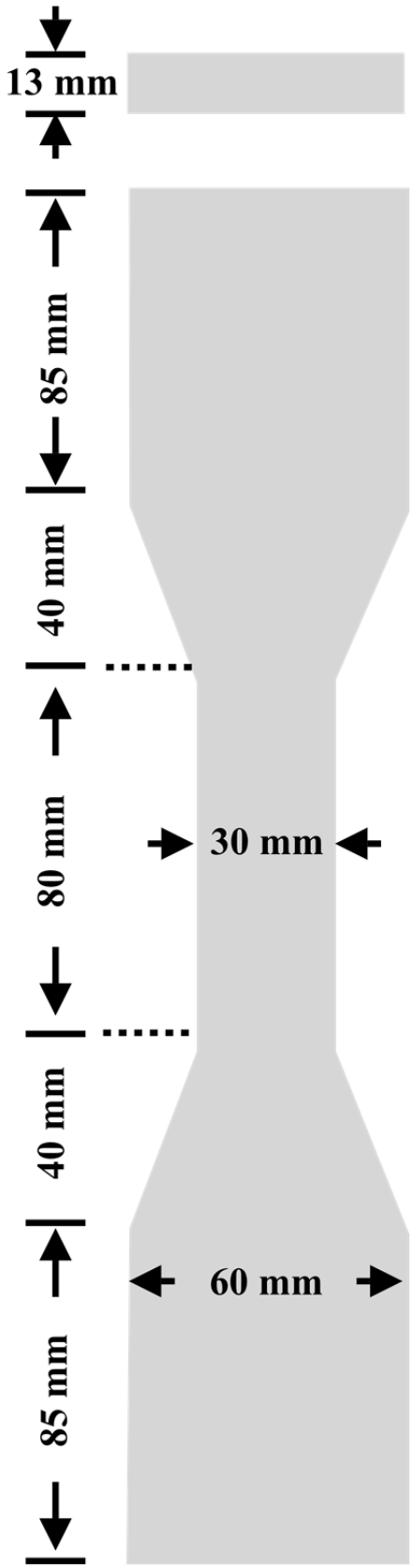

Figure 2b
Click here to download Figure: Figure 2b.pdf

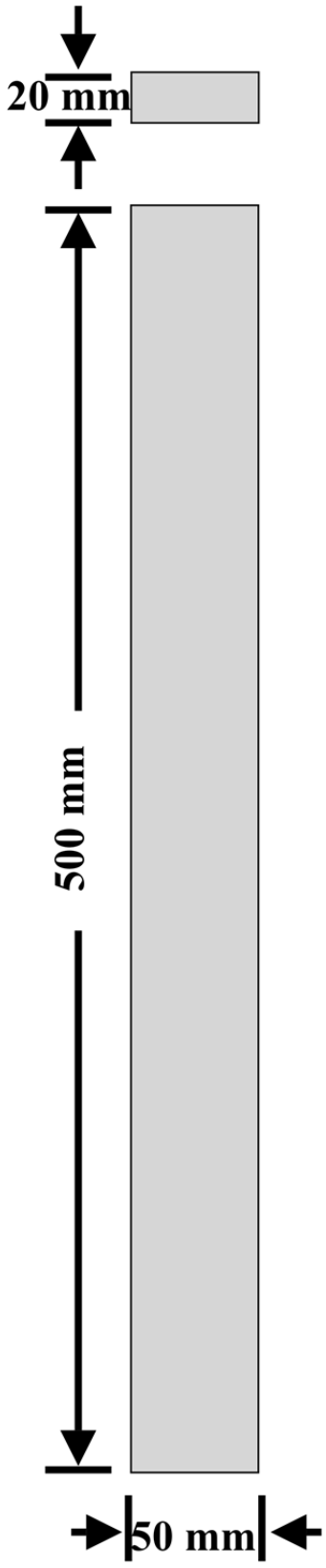

Figure 2c
Click here to download Figure: Figure 2c.pdf

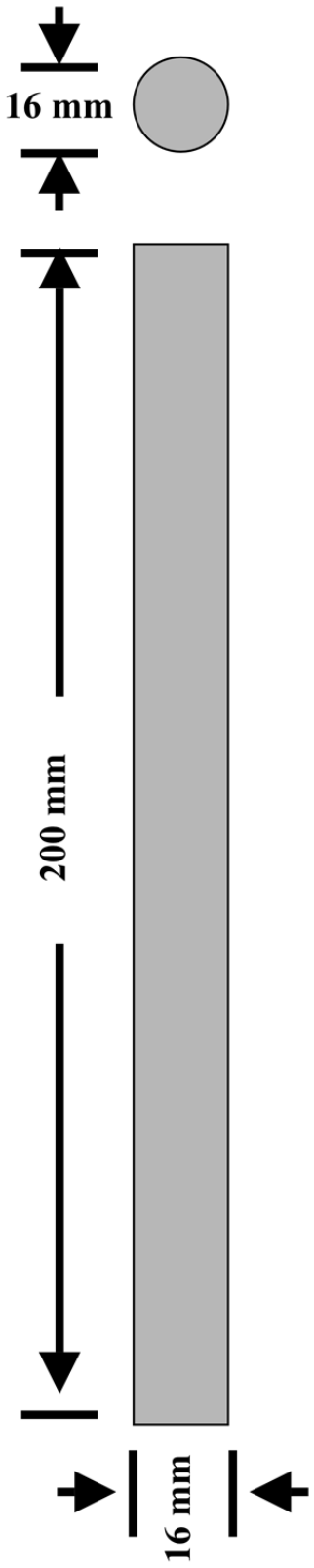

Figure 3
Click here to download Figure: Figure 3.pdf

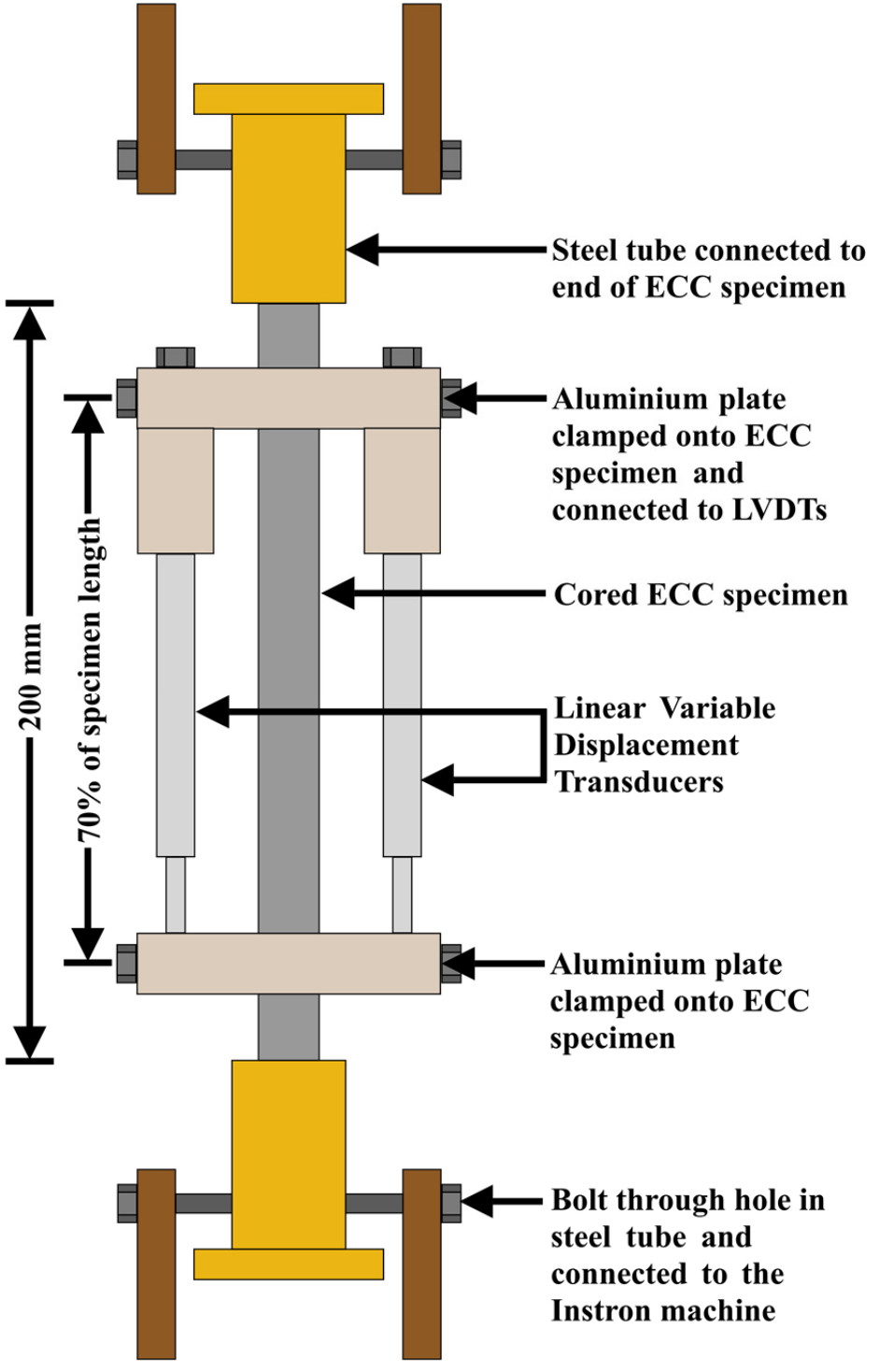

Figure 4a

Click here to download Figure: Figure 4a.pdf

Figure 4b
Click here to download Figure: Figure 4b.pdf

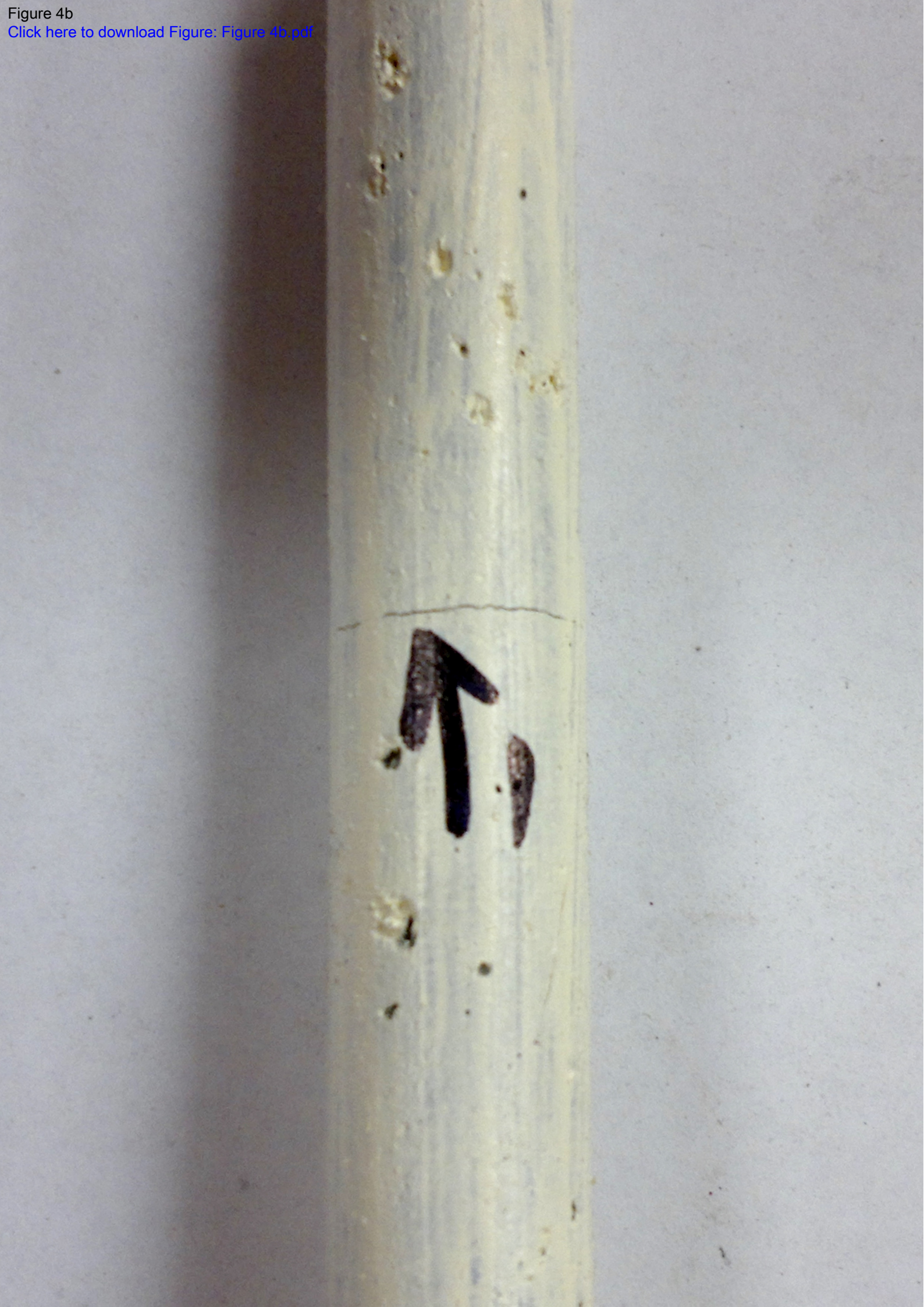

Figure 5a
Click here to download Figure: Figure 5a.pdf

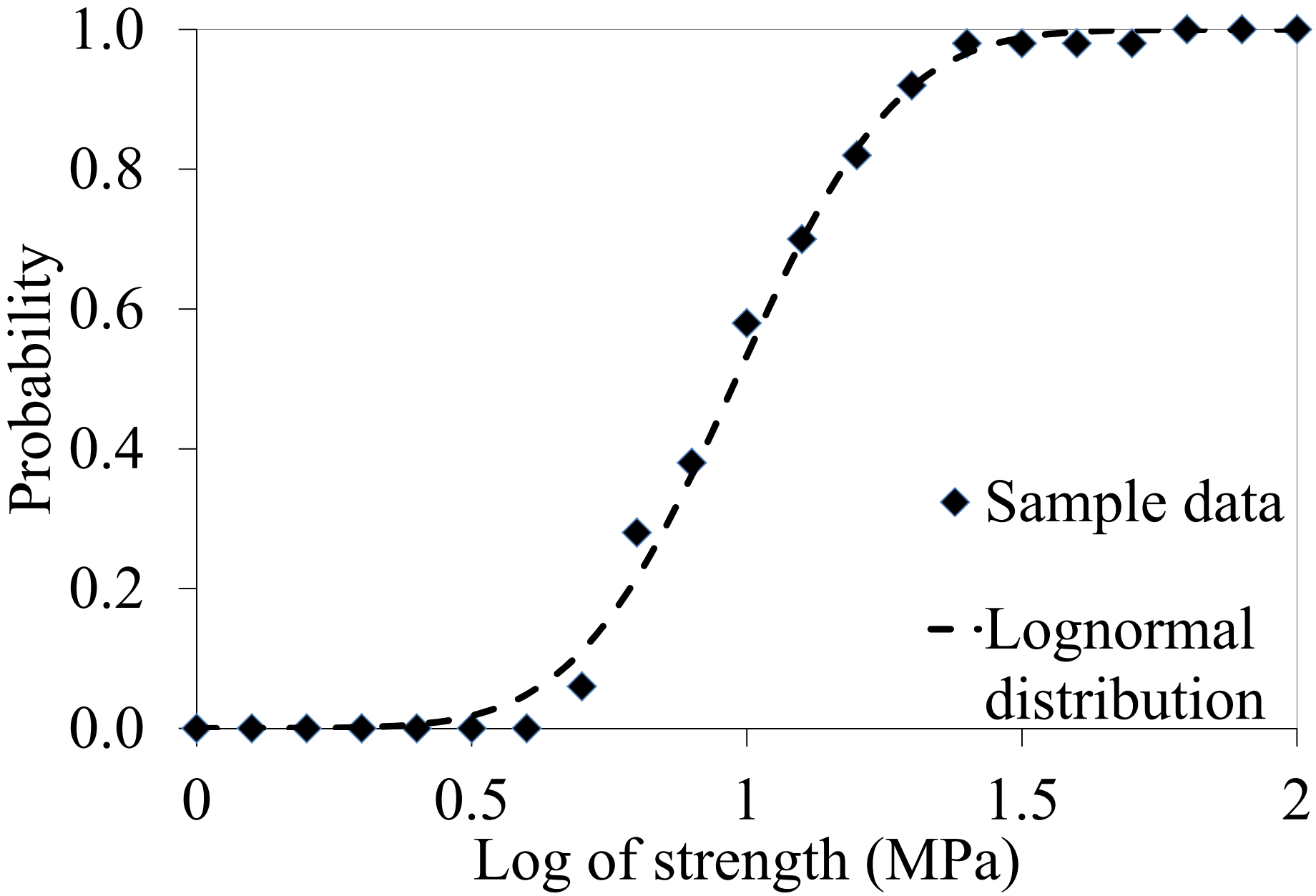

Figure 5b
Click here to download Figure: Figure 5b.pdf

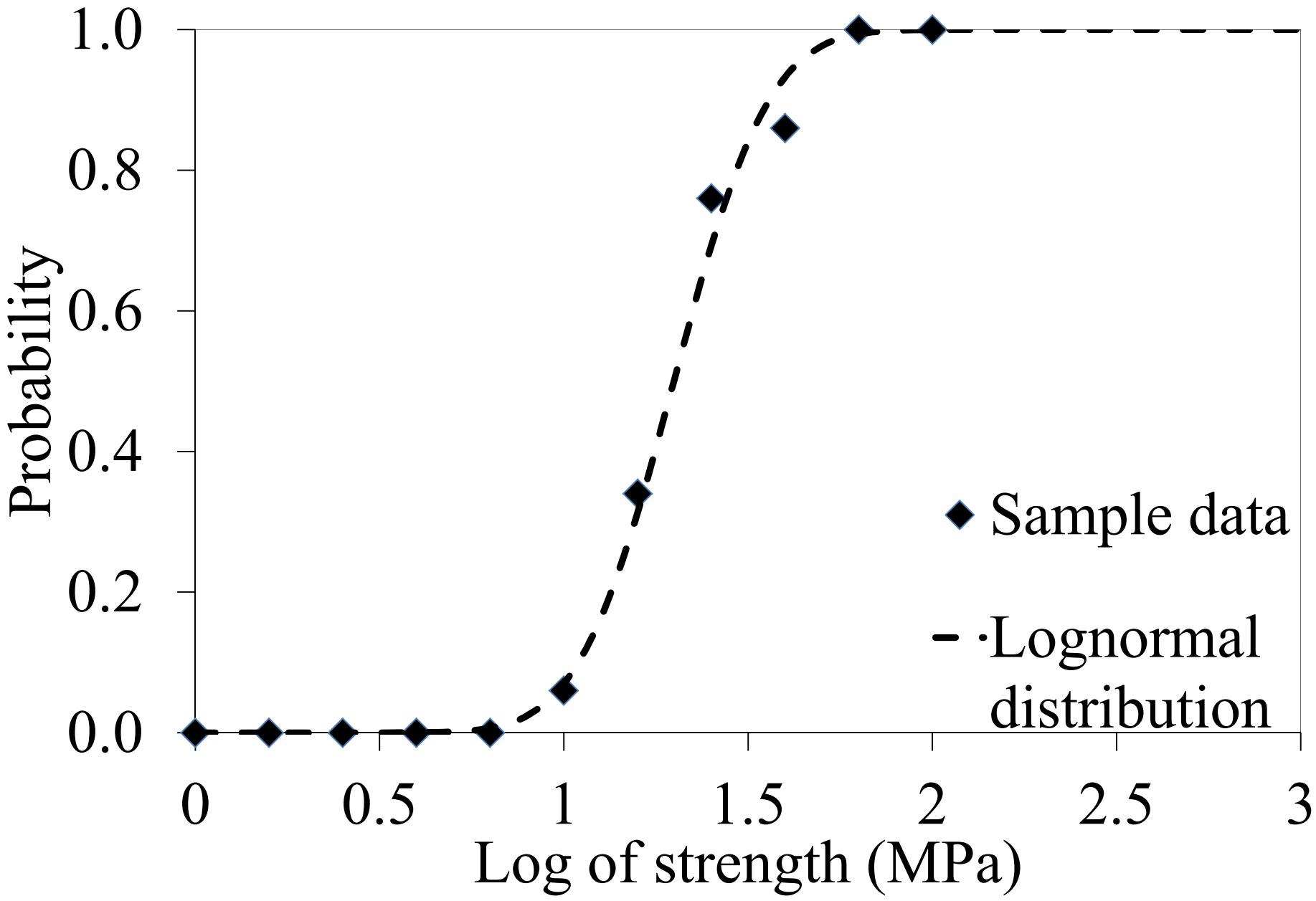

Figure 5c
Click here to download Figure: Figure 5c.pdf

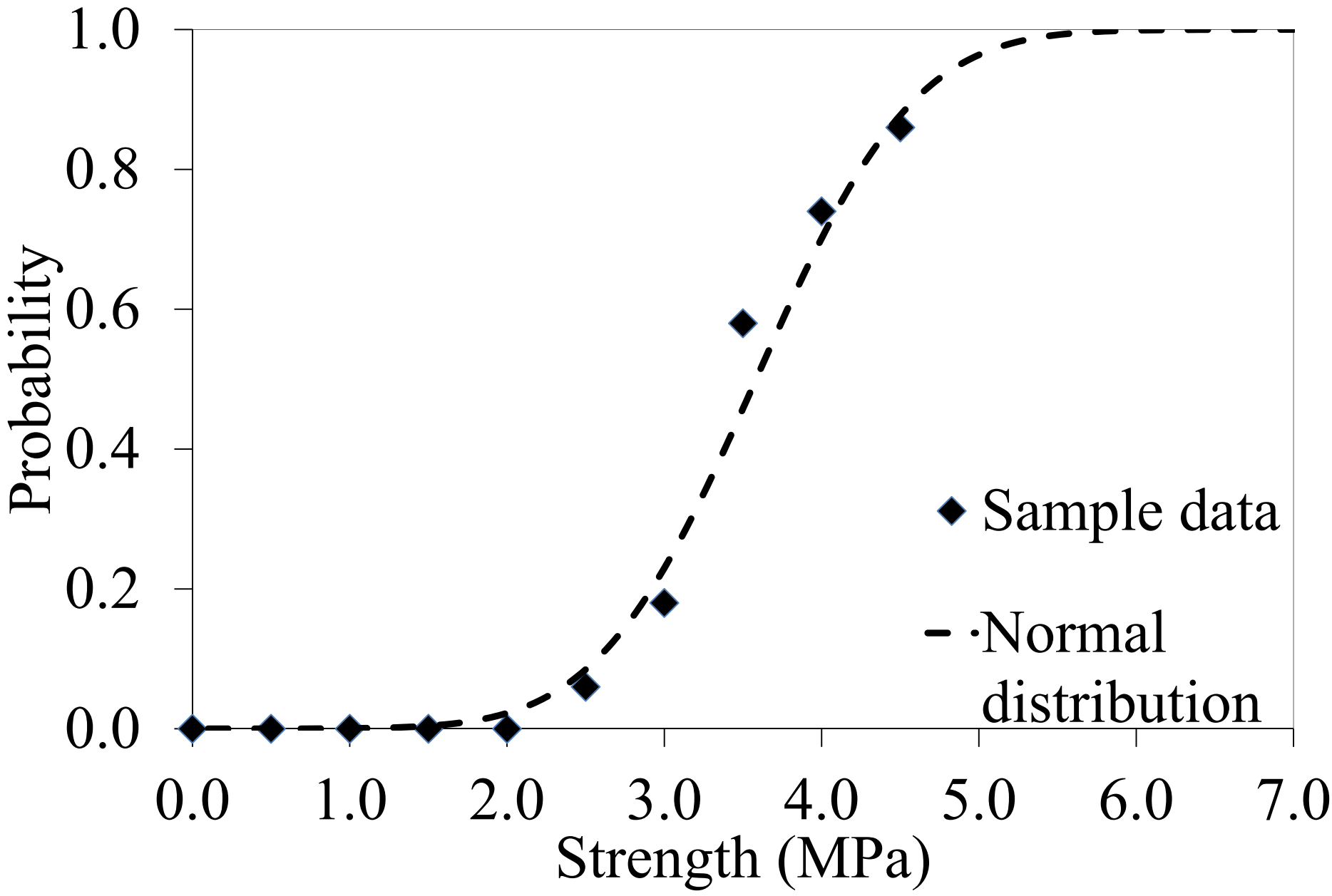

Figure 6a
Click here to download Figure: Figure 6a.pdf

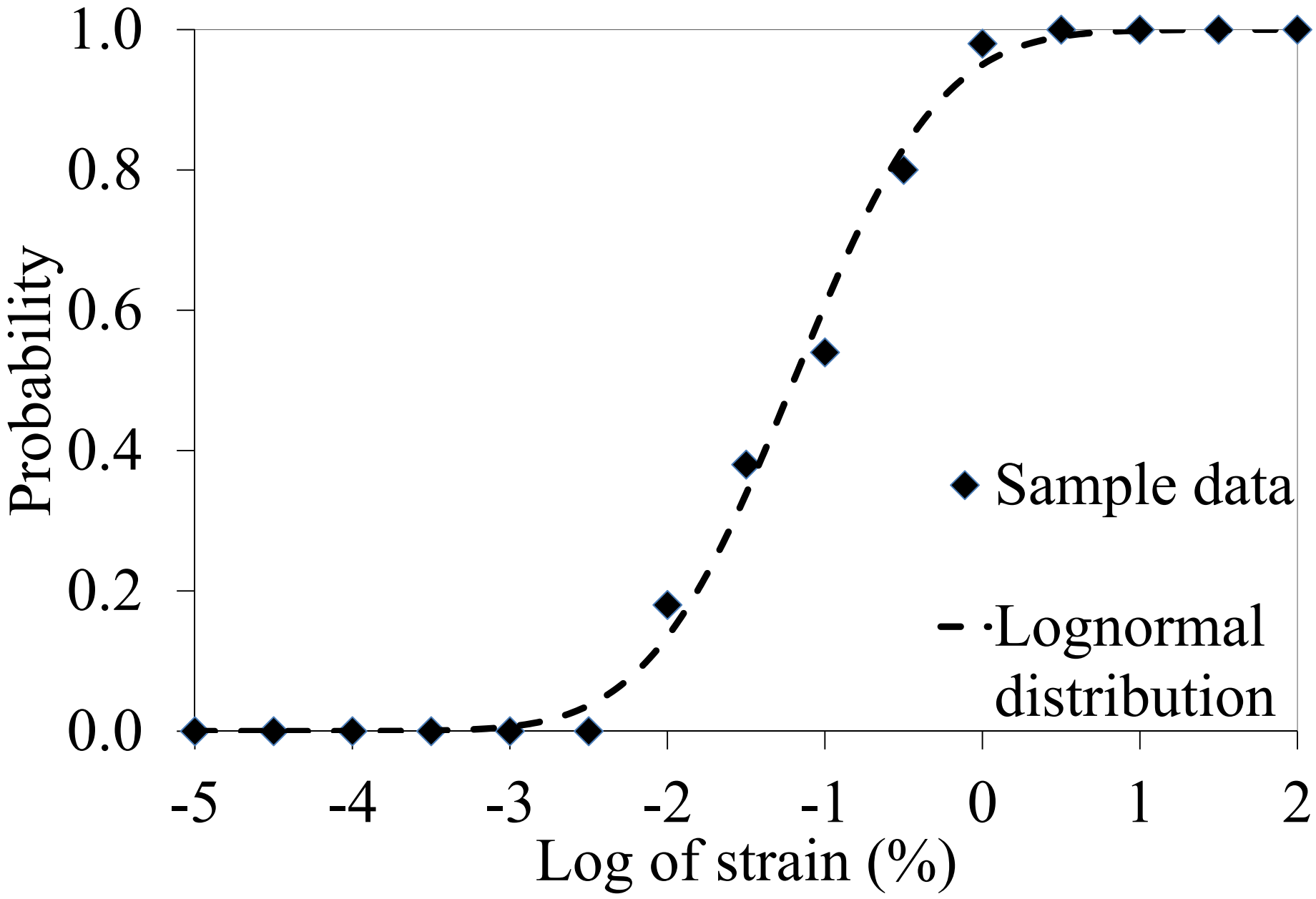

Figure 6b
Click here to download Figure: Figure 6b.pdf

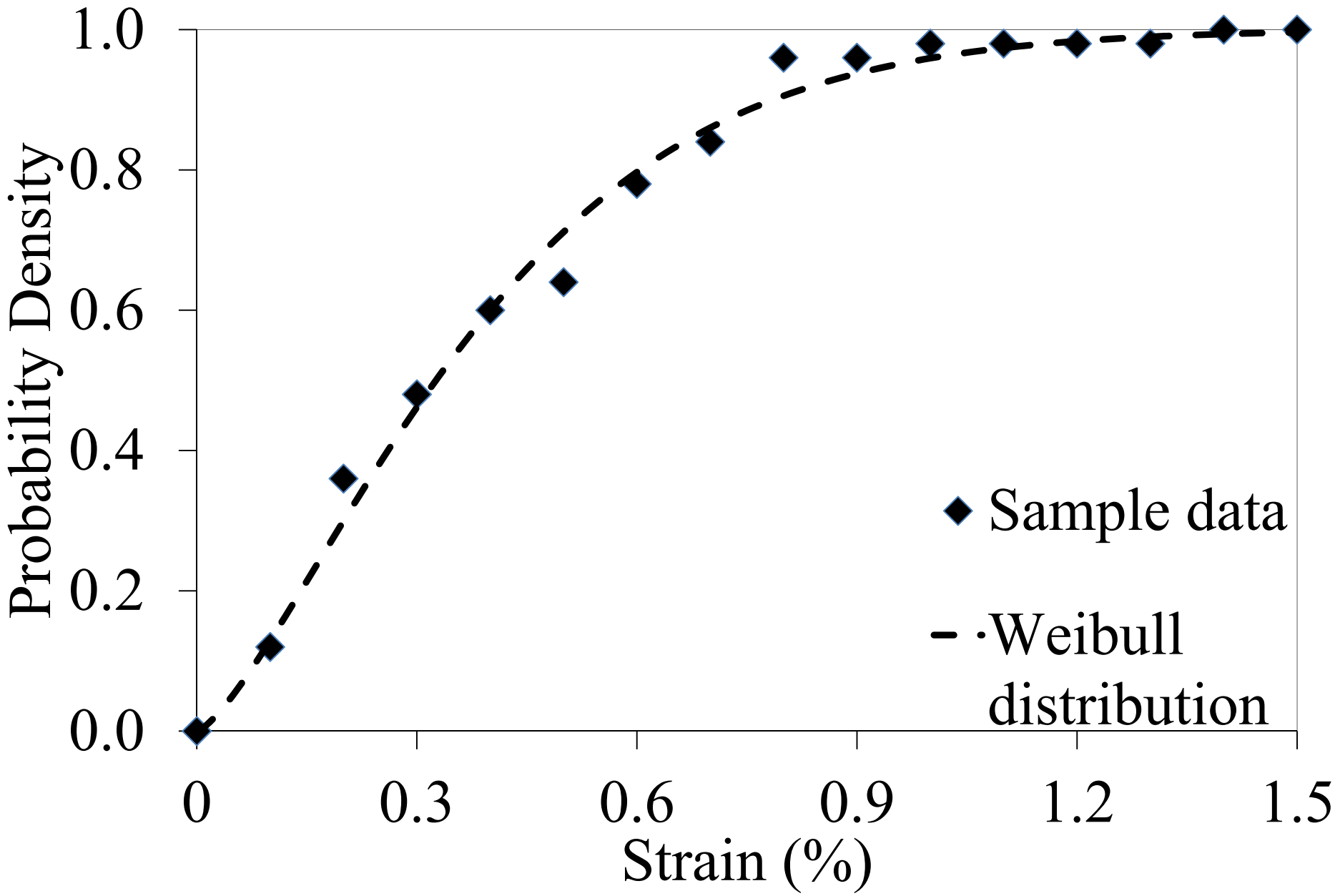

Figure 6c
Click here to download Figure: Figure 6c.pdf

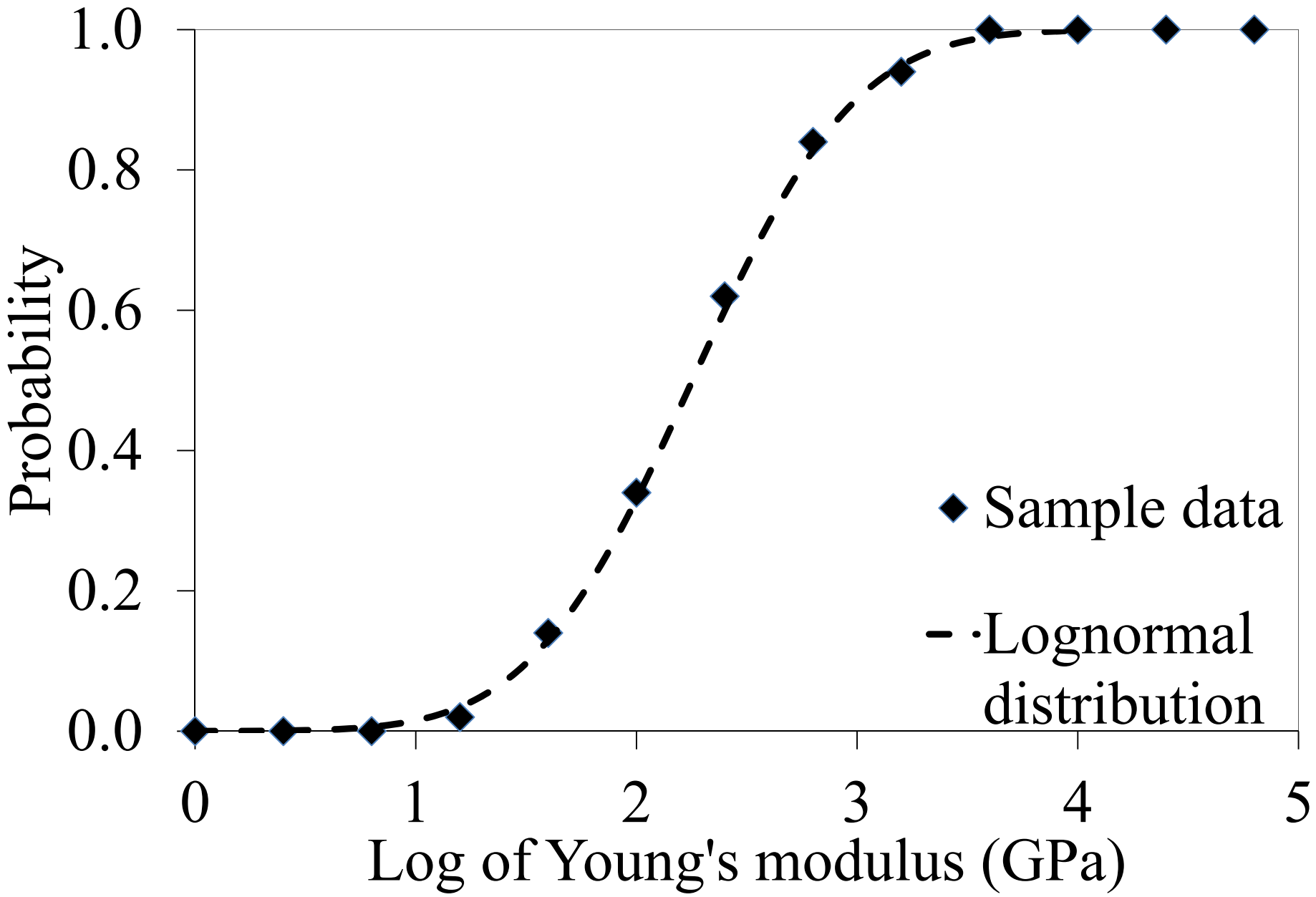

Figure 7
Click here to download Figure: Figure 7.pdf

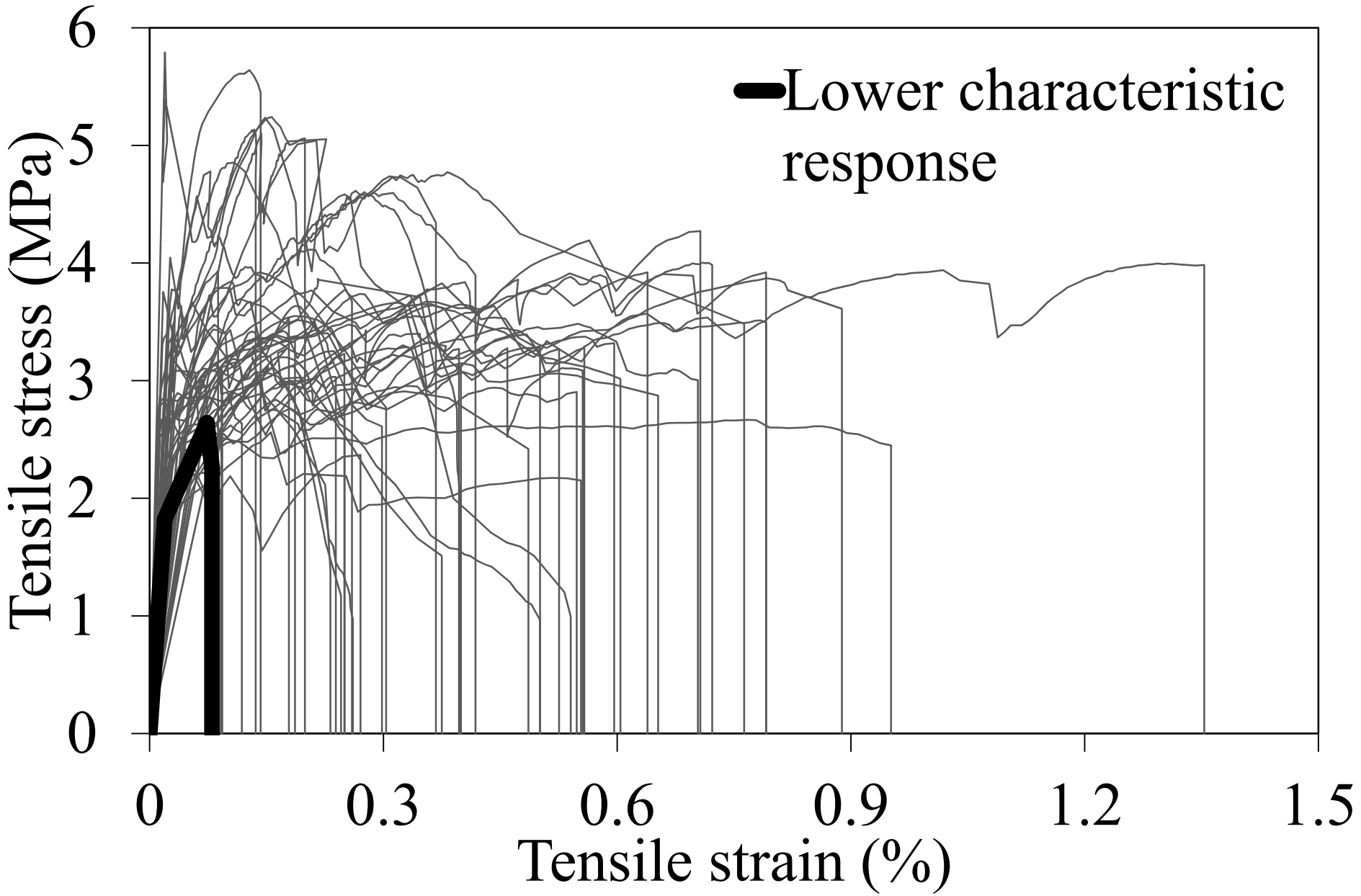

Figure 8
Click here to download Figure: Figure 8.pdf